

FORM OF A LIQUID LAYER OF CONSTANT MASS ON THE SURFACE  
OF A ROTATING CYLINDER

V. E. Epikhin, P. N. Konon, and V. Ya. Shkadov

UDC 532.516

Comparison with experimental data reveals satisfactory agreement of results of a theoretical study of the equilibrium form and hydrodynamic stability of a liquid layer on the surface of a rotating horizontal cylinder.

The phenomenon of instability of the free surface of a liquid is observed in many technological processes [1, 2]. Theoretical study of nontrivial equilibrium forms after loss of stability in liquid jets and layers of cylindrical form rotating like a solid were carried out by the small parameter method in [3-6]. The method of extending the analytical solution was used in [7]. Below we will establish the relationship between the form of the free surface of a rotating layer and the pressure head in the liquid and surrounding medium with no assumption of smallness of the deviation of nontrivial equilibrium surfaces from cylindrical. It will be shown that after loss of stability for certain values of the pressure head equilibrium periodic layers with various orders of symmetry are formed. Comparison with the experimental data of [2] shows that in reality one does find nonsteady state periodic disturbances of the cylindrical free surface having the largest increment coefficient in linear hydrodynamic stability theory.

1. Neglecting viscous interaction with the surrounding medium and mass forces, in the cylindrical coordinate system  $\{r, z, \theta\}$  fixed to the rotating cylinder, one can derive the equation of the surface of the viscous liquid layer  $r = h(z, \theta)$  fixed relative to the surface of the rotating cylinder [4, 5]. In the case  $r = h(\theta)$  this equation transforms to the form [8]

$$2hh'' - 4(h')^2 + We(2Eu - 1 + h^2)[(h')^2 + h^2]^{3/2} - 2h^2 = 0. \quad (1)$$

Equation (1) is supplemented by periodicity conditions along  $\theta$  and a condition expressing the conservation of mass  $m_*$  within the layer:

$$h(0) = h(2\pi), \quad h'(0) = h'(2\pi), \quad (2)$$

$$\frac{1}{2} \int_0^{2\pi} (h^2 - 1) d\theta = m_* = \pi (h_s^2 - 1). \quad (3)$$

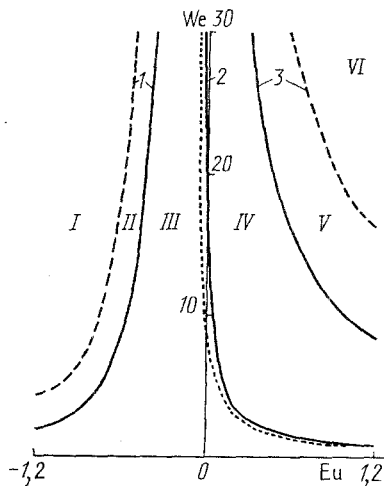


Fig. 1. Division of the parameter plane  $(Eu, We)$  into subregions.

TABLE 1. Number of Real Roots of the Polynomials  $Q_0, Q_1, Q_2$  in Various Subregions

Number of real polynomial roots greater than unity	Subregion number					
	I	II	III	IV	V	VI
$N_0$	2	2	0	0	1	1
$N_1$	2	0	0	0	0	1
$N_2$	2	2	2	1	1	1

As was shown in [8], the first integral of Eq. (1) has the form

$$(h')^2 = -h^2 Q_1 Q_2 / Q_0^2, \quad (4)$$

$$Q_0(h, B) = h^4 + 2(2Eu - 1)h^2 - B, \quad Q_n(h, B) = Q_0 - (-1)^n 8h/We,$$

$$n = 1, 2.$$

The layer surface extrema are given by the roots of the polynomials  $Q_1, Q_2$ , which are larger than unity. The root of the polynomial  $Q_0$  is a singular point, since if as  $h \rightarrow h_*$  the polynomial  $Q_0 \rightarrow 0$ , then the derivative  $|h'| \rightarrow \infty$ . A study of the number of real roots of the polynomials  $Q_0, Q_1$ , and  $Q_2$ , greater than unity in the plane of the parameters  $(Eu, We)$ , was performed by the Shturm method in the semiinfinite band  $-1.2 \leq Eu \leq 1.2; We > 0$ . The region to be studied was covered by a grid of points with coordinates  $Eu_m = -1.2 + (m - 1) \cdot 0.01; We_k = k \cdot 0.1; m = 1, 2, \dots, M; k = 1, 2, \dots, K$ . The roots of the polynomial were studied for each pair of numbers  $(m, k)$ . In Fig. 1 the solid and dashed lines 1, 2, 3 divide the region under study into subregions I, II, III, IV, V, VI, in which the polynomials  $Q_0, Q_1, Q_2$  have a fixed number of real roots  $N_0, N_1, N_2$  greater than unity. Values of  $N_0, N_1, N_2$  are shown in Table 1. The dashed curve of Fig. 1 shows the relationship of the parameters  $Eu_0$  and  $We$  for the case of a layer of constant thickness  $h_0 = 1.1$ . At parameter values in subregion I the layer surface has two vertical and two horizontal tangents per wavelength; in subregion II, four vertical and two horizontal; III, two horizontal; IV, one horizontal; V, one horizontal and two vertical. In subregions I, II, III, VI the layer is continuous, while in IV and V it consists of isolated masses. The dashed curve passes through subregion III such that at small deviations of the parameters  $Eu$  and  $We$  from an equilibrium cylindrical layer equilibrium wavelike surfaces or isolated masses which do not intersect develop.

2. We will consider the method of solving the boundary problem including Eq. (1) and supplemental conditions (2), (3), which will be considered as a system of three nonlinear equations with the three unknowns  $Eu, h(0), h'(0)$ :

$$\Phi_1 [Eu, h(0), h'(0)] = \frac{1}{2} \int_0^{2\pi} (h^2 - 1) d\theta - m_* = 0, \quad (5)$$

$$\Phi_2 [Eu, h(0), h'(0)] = h(0) - h(2\pi) = 0, \quad \Phi_3 [Eu, h(0), h'(0)] = h'(0) - h'(2\pi) = 0.$$

System (5) can be solved numerically. In the first stage for the initial approximation we use the value  $Eu = Eu_0$ , corresponding to a layer of constant thickness, with the derivative  $h'(0) = 0$ , while for the initial approximation of  $h(0)$  we use successively the values  $1, 1 + \Delta h_0, 1 + 2\Delta h_0, \dots, 1 + K\Delta h_0 = h_0$ , where  $\Delta h_0$  is the step into which the interval  $[1,$

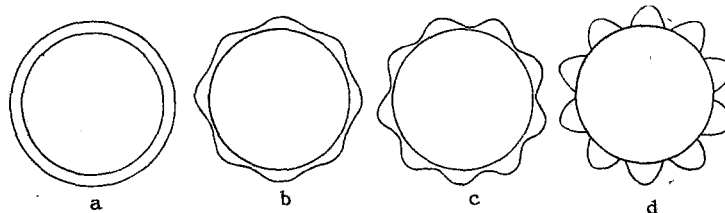


Fig. 2. Layer free surface forms at  $m_* = 0.85; We = 44$ :  
a)  $Eu = Eu_0 = -0.1142$ ; b)  $-0.1162$ ; c)  $-0.1239$ ; d)  $-0.1286$ .

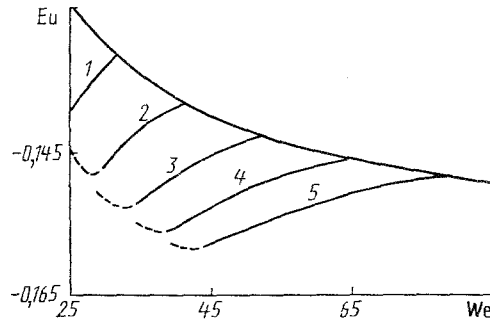


Fig. 3. Branching of the curves  $Eu_n(We)$  from curve  $Eu_0(We)$  at  $m_* = 1$ : 1)  $n = 7$ ; 2) 8; 3) 9; 4) 10; 5) 11.

$h_0]$  is divided. Equation (1) is integrated over the interval  $[0, 2\pi]$  with corresponding initial conditions by the Runge-Kutta method with fourth order accuracy formulas. Then Eq. (5) is calculated. New  $h(0)$  values are chosen until the inequality

$$\max |\Phi_l| \leq \varepsilon, \quad l = 1, 2, 3 \quad (6)$$

is satisfied. For  $\varepsilon$  the value  $5 \cdot 10^{-2}$ ,  $\Delta h_0 = 0.1(h_0 - 1)$  was chosen. In the second stage the method of successive approximations in Newton's form was used. The values of the unknowns obtained in the first stage were used as initial approximations. The calculation process was then continued until satisfaction of Eq. (6), in which  $\varepsilon = 10^{-4}$ .

Figure 2 shows the forms of the free surface of the layer, with  $m_*$  and  $We$  specified. The solution of Eqs. (1)-(3) is not unique, since the various values of the number  $Eu$  correspond to layers with various orders of symmetry  $n$ . Figure 3 shows the branching of the curves  $Eu_n(We)$  from the curve  $Eu_0(We)$ , corresponding to a layer of constant thickness. Thus, specification of the parameters  $We$  and  $m_*$  is not sufficient to define the pressure head in the liquid and surrounding medium, as well as the form of the layer free surface.

The linear theory of hydrodynamic stability [9] will allow us to obtain necessary and sufficient conditions for stability of a cylindrical layer of constant thickness with respect to infinitely long disturbances parallel to the directrix of the rigid cylinder, the normal sections of which have  $n$ -th order symmetry, and in particular, in the case of an ideal liquid

$$We \leq \frac{n^2 - 1}{h_0^3(1 - a_n/n)}, \quad 0 < a_n = \frac{h_0^{2n} - 1}{h_0^{2n} + 1}, \quad n \geq 2;$$

and for a viscous liquid

$$We \leq We_n = (n^2 - 1)/h_0^3. \quad (7)$$

TABLE 2. Comparison of Experimental Data with Calculations by Linear Hydrodynamic Instability Theory

$R_0$	$\omega_0$	$We$	Data of [2]		Calc. results		
			$h_s$	$n_s$	instability region	$n$	$(n-n) \cdot 100\%$
0,0123	25,13	21,15	1,134	4	$n \leq 5$	4	0
0,025	18,85	99,9	1,136	4-6	11	8	37,5
0,025	25,13	177,7	1,081	7-9	15	10	10
0,025	33,51	315,8	1,056	9-11	19	13	15,3
0,035	18,85	274,2	1,069	7-9	18	12	25
0,035	25,13	487,5	1,053	12-13	23	16	18,8
0,035	33,51	866,6	1,033	14-16	30	21	33,3
0,035	41,89	1354	1,028	17-19	38	26	34,6

If, for example,  $We_N < We < We_{N+1}$ , then disturbances at  $n \leq N$  are unstable, while those with  $n > N$  are stable. The square of the unstable disturbance increment for the case of an ideal liquid has the form

$$C_{i_1}^2 = a_n [n(1 - We_n/We) - a_n] > 0. \quad (8)$$

The right side of Eq. (8) vanishes at  $n = 0$  and is less than zero for  $n = N + 1$ . Therefore, at some intermediate value  $n$  ( $0 < n < N + 1$ ) the increment has a maximum. It can be expected that the perturbation corresponding to this  $n$  will be the most unstable, as is, other conditions being equal, realized in experiments. Table 2 shows data of [2], results of defining instability regions with consideration of Eq. (7), and the modes with most rapid increment, determined with consideration of Eq. (8). The rightmost column shows the relative divergence between the calculated and experimentally observed modes, which does not exceed 38%, and can be explained by the idealization of the real layer form and nonconsideration of viscosity. This fact permits the conclusion that in experiment perturbations were observed, corresponding to modes periodic in angle, increasing with time.

Conclusion. Results of a numerical study of equilibrium form and hydrodynamic stability of a layer rotating as a solid have been presented, with consideration of centrifugal acceleration and liquid surface tension. Specification of the Weber number and the liquid mass in the layer are insufficient to determine the pressure head in the liquid and surrounding medium, as well as the form of the layer free surface. Comparison with experimental data shows that in reality nonsteady state disturbances of the layer free surface are observed, corresponding to modes periodic in angle, having the highest increment, as defined by linear theory.

#### NOTATION

Dimensionless parameters of the problem: Weber number  $We = \rho R_0^3 \omega_0^2 / \sigma$ ; Euler number  $Eu = (P_1 - P_0) / (\rho \omega_0^2 R_2^0)$ ;  $\rho$ , liquid density;  $R_0$ , cylinder radius;  $\omega_0$ , angular velocity of cylinder rotation;  $\sigma$ , liquid surface tension coefficient;  $P_1$ , pressure in liquid at cylinder surface;  $P_0$ , pressure of undisturbed surrounding medium;  $h_s$ , mean weighted layer thickness;  $B$ , integration constant.

#### LITERATURE CITED

1. G. F. Tobol'skii, Mineral Wool and Parts Made Thereof [in Russian], Chelyabinsk (1968).
2. A. E. Kulago, V. P. Myasnikov, V. G. Petrov-Denisov, and A. M. Pichkov, Construction and Production of Special Equipment [in Russian], Moscow (1981), pp. 76-84.
3. C. S. Yih, Proc. R. Soc., A258, 63-86 (1960).
4. V. V. Pukhnachev, Zh. Prikl. Mekh. Tekh. Fiz., No. 2, 127-134 (1973).
5. Yu. K. Bratukhin and L. N. Maurin, Prikl. Mat. Mekh., No. 4, 754-756 (1968).
6. L. D. Myshkis (ed.), Hydrodynamics of Weightlessness [in Russian], Moscow (1976).
7. L. G. Badratinova, Zh. Prikl. Mekh. Tekh. Fiz., No. 4, 56-59 (1981).
8. V. E. Epikhin, P. N. Konon, and V. Ya. Shkadov, Inzh.-Fiz. Zh., 55, No. 3, 423-431 (1988).
9. J. Gillis and K. S. Suh, Phys. Fluids, 5, No. 10, 1149-1155 (1962).